

DAVIDE FUGAZZA(*), ANTONELLA SENESE(*), ROBERTO SERGIO AZZONI(*),
CLAUDIO SMIRAGLIA(*), MASSIMO CERNUSCHI(**),
DAVIDE SEVERI(**) & GUGLIELMINA ADELE DIOLAIUTI(*)

HIGH-RESOLUTION MAPPING OF GLACIER SURFACE FEATURES. THE UAV SURVEY OF THE FORNI GLACIER (STELVIO NATIONAL PARK, ITALY)

ABSTRACT: D. FUGAZZA, A. SENESE, R.S. AZZONI, C. SMIRAGLIA, M. CERNUSCHI, D. SEVERI & G. A. DIOLAIUTI. *High resolution mapping of glacier surface features. The UAV survey of the Forni Glacier (Stelvio National Park, Italy)* (IT ISSN 0391-9838, 2015).

Fast, reliable and accurate methods for glacier mapping are necessary for understanding glacier dynamics and evolution and assessing their response to climate change. Conventional semi-automatic approaches are based on medium-resolution satellite images, but their use can cause significant loss of accuracy when analyzing small glaciers, which are predominant in the Alps. In this paper, we present a semi-automatic segmentation approach based on very high-resolution visible RGB images acquired from a UAV (Unmanned Aerial Vehicle) survey of the Forni Glacier, in the Italian Alps, using an off-the-shelf digital camera. The method has the ability to map large-scale morphological features, i.e. bare ice and medial moraines, with better accuracy than methods relying on medium-resolution satellite imagery, with only slight misclassification at the margins. By using segmentation, we also mapped small-scale morphologies not discernible on satellite images, including epiglacial lakes and snow patches, in a semi-automatic way. On a small portion of the eastern ablation tongue, featuring homogeneous illumination conditions, we also investigated in finer detail the occurrence of fine and sparse debris and tested a texture filter technique for mapping crevasses, which showed promising results. Our analyses confirm that the glacier is un-

dergoing intense dynamic processes, including darkening of the ablation tongue and increased surface instability, and show the potential of UAVs to revolutionize glaciological studies. We suggest that by using a combination of different payloads, mapping of glacier features via UAVs could reach high levels of accuracy and speed, making them useful tools for glacier inventories and geomorphological maps.

KEY WORDS: High resolution mapping, Remote sensing, UAV (Unmanned Aerial Vehicle), Alpine glaciers, Forni Glacier, Italy.

RIASSUNTO: D. FUGAZZA, A. SENESE, R.S. AZZONI, C. SMIRAGLIA, M. CERNUSCHI, D. SEVERI & G. A. DIOLAIUTI. *Cartografia ad alta risoluzione della superficie glaciale e delle sue forme. Il rilievo tramite drone del Ghiacciaio dei Forni (Parco Nazionale dello Stelvio, Italia)*. (IT ISSN 0391-9838, 2015).

La cartografia delle superfici glaciali richiede l'utilizzo di metodi veloci, precisi e affidabili, per meglio comprendere le dinamiche glaciali, i processi evolutivi e la risposta dei ghiacciai ai cambiamenti climatici. L'uso di approcci semi-automatici tradizionali, basato su immagini satellitari alle medie risoluzioni, può causare notevoli perdite di precisione nell'analisi di corpi glaciali di piccole dimensioni, che costituiscono la maggior parte dei glacialismo alpino. In questo studio, presentiamo un nuovo approccio semi-automatico basato sulla segmentazione di immagini ad altissima risoluzione acquisite tramite fotocamera digitale durante un rilievo del Ghiacciaio dei Forni (Parco Nazionale dello Stelvio, Italia), effettuato con un drone (Aeromobile a Pilotaggio Remoto). Con questo metodo è stato possibile cartografare forme a grande scala, ovvero ghiaccio esposto e morene mediane, con maggiore precisione rispetto ai metodi basati su immagini satellitari a media risoluzione, nonostante alcuni trascurabili errori di classificazione ai margini del ghiacciaio. L'uso della segmentazione ha permesso anche la cartografia semi-automatica di forme a piccola scala, non visibili da immagini satellitari, inclusi laghi epiglaciali e nevai. Su una porzione ridotta della lingua d'ablazione orientale, caratterizzata da condizioni di illuminazione uniforme nelle immagini, abbiamo inoltre indagato con maggiore dettaglio la presenza di detrito fine e sparso e sperimentato un filtro d'immagine basato sulle *texture* per cartografare i crepacci, con risultati molto incoraggianti. Le analisi forniscono una conferma degli intensi processi dinamici a cui è sottoposto il ghiacciaio, come la sempre maggiore presenza di detrito sulla lingua d'ablazione e un incremento di instabilità superficiale, e dimostrano le potenzialità dei droni per innovare gli studi glaciologici. Attraverso la combinazione di diversi

(*) Dipartimento di Scienze della Terra, Università degli Studi di Milano.

(**) Agricola 2000 S.c.p.A., Milano.

(*) corresponding authors: davide.fugazza@yandex.com, guglielmina.diolaiuti@unimi.it

The research was performed under the umbrella of an agreement between the Università degli Studi di Milano and Sanpellegrino SpA brand Levisissima. Moreover the Agricola 2000 S.c.p.A supported this study taking part with their UAV to the field investigations and also participating to the Lab analysis. The authors kindly acknowledge the Stelvio National Park managers and staff for their help and support. This work was also performed in the framework of the PRIN project 2010/2011 (2010AYKTAB_006), local leader C. Smiraglia. The results of this research also represent a contribution to the development of the updated guidelines of the New Italian Geomorphological Map under the umbrella of the AIGEO working group devoted to this issue.

sensori, la cartografia delle superfici glaciali tramite droni potrebbe in futuro raggiungere elevati livelli di precisione e rapidità, risultando così uno strumento utile per i catasti glaciali e la cartografia geomorfologica.

TERMINI CHIAVE: Cartografia ad alta risoluzione, Telerilevamento, Drone - APR (Aeromobile a Pilotaggio Remoto), Ghiacciai alpini, Ghiacciaio dei Forni, Italia.

INTRODUCTION

Retreat of glaciers worldwide since the Little Ice Age is one of the clearest clues of climate change. In the Alps, glacier shrinkage has been particularly severe since the 1980s and if the trend continues, many Alpine glaciers could disappear during the 21st century, with a serious impact on the energy and water supply (EEA, 2012). During its active phase, glacier recession is also followed by geomorphological changes such as an increase in supraglacial debris cover and formation of epiglacial lakes (Diolaiuti & Smiraglia, 2010). Debris cover affects ice albedo and plays an important role in the glacier energy balance (Oerlemans & alii, 2009), while ice-contact lakes can increase ice ablation via calving processes (Benn & alii, 2012).

Fast and reliable methods for glacier mapping are necessary to study the evolution of glaciers and assess their response to climate change. For this purpose, several semi-automatic approaches employing medium-resolution satellite imagery such as ASTER and Landsat (15-30 m of pixel resolution) have been developed, using a combination of optical, thermal and/or morphometric data (for a review see Shukla & alii, 2010). Accuracy of medium-resolution methods, however, decreases when analyzing changes in smaller glaciers (Paul & alii, 2013). This precludes mapping of small-scale geomorphological features, including crevasses, snow patches and small epiglacial lakes, and of fine and sparse debris, which is widespread on most glaciers and likewise has an impact on the albedo (Azzoni & alii, 2014).

In theory, images with higher resolution could provide a more detailed discrimination of supraglacial features. High-resolution satellite imagery however is available at a high cost to the end users, and so far it has mainly been employed as a means of validating lower resolution methods, substituting fieldwork. In glacier inventories, orthomosaics from aerial surveys are also employed for mapping glacier boundaries via manual delineation, as in the recently developed Swiss Glacier inventory (Fischer & alii, 2014). However, this process is slow and further information is usually needed to identify glacier margins on highly debris-covered glaciers. A semi-automatic approach, developed by Knoll & Kerschner (2009) for the Tyrol Inventory, was based on Airborne Laser Scanning (ALS) surveys, but whenever it was applied over debris-covered glaciers manual correction was required. ALS surveys are also expensive, and this limits their application on a global scale.

More recently, unmanned aerial vehicles (UAV) have been introduced to the field of glacier studies. These enable low cost on-demand inspection of relatively wide areas of interest, with the ability to carry different types of payload (e.g. a digital camera, near-infrared or thermal sensor) and to survey an area with a better resolution than commercial satellites. UAV-derived orthomosaics have been used to analyze specific features such as cryoconite holes and granules, in combination with ground photography (Hodson & alii, 2007), supraglacial lakes (Immerzeel & alii, 2014), and crevasses, mapped by Ryan & alii (2015) via manual delineation. In this paper, we assess the feasibility of mapping several glacier features (i.e. snow, buried- and bare-ice, epiglacial lakes, and crevasses) of the Forni Glacier from a UAV high-resolution orthomosaic produced using an off-the-shelf digital camera with a semi-automatic approach. In addition, we investigate in more detail these glacier features analyzing a smaller area along the Forni Glacier ablation tongue featuring homogeneous illumination conditions. Finally, to evaluate the advantages provided by this methodology we compare it to classification based on medium-resolution data acquired by Landsat 8.

STUDY AREA

The Forni Glacier is part of the Ortles-Cevedale group, Lombardy Alps, and of the Stelvio National Park (fig. 1). It is the widest Italian valley glacier (ca. 11.36 km²; D'Agata & alii, 2014), with a northerly aspect and an elevation range between 3670 and 2600 m. It is a composite glacier, formed by three ice streams joining into a tongue that extends for ca. 2 km. Two medial moraines are located on the tongue, originating from rock outcrops located below the snow line and nourished by supra-glacial debris derived from valley rocks (Smiraglia, 1989). The ablation tongue is mostly debris-free, although a recent increase in fine and sparse debris deposition due to the ongoing glacier shrinkage has been reported (Diolaiuti & Smiraglia, 2010; Senese & alii, 2012a). Other considerable morphological changes have lately taken place, including the appearance of debris cones, epiglacial ponds and the formation of neo-moraines. Owing to this diverse range of glacial features, together with the ease of access and the long series of volume, area and length dataset, the Forni Glacier is an ideal ground for evaluating our methodology.

METHODS

The methodology proposed in this study aims at classifying both large-scale and small-scale features on the surface of the Forni Glacier ablation tongue. We consider as large-scale features the main glacier body and the medial moraines. These are much larger than a Landsat pixel, and

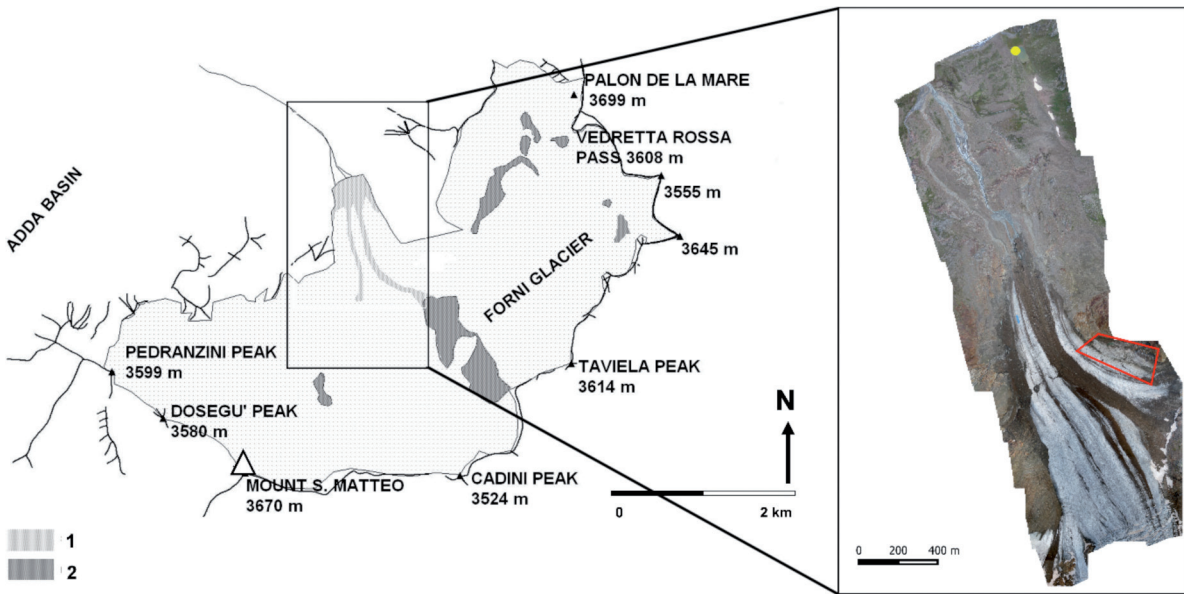


FIG. 1 - (A) Map of the Forni Glacier from aerial orthophoto acquired in 2003: medial moraines and supraglacial debris are indicated in light-grey (1), and nunataks are highlighted in dark-grey (2). (B) Area imaged by the UAV in August 2014: the yellow dot displays the UAV launch and landing location, while the area investigated in higher detail is shown as the red box.

thus clearly identifiable on both Landsat and UAV images. It follows that small-scale features are those smaller than a Landsat pixel, and we considered among them debris-rich ice, snow-patches, epiglacial lakes and crevasses.

DATA SOURCES

The UAV used in this study was SwingletCAM, built by SenseFly. SwingletCAM is a fixed-wing UAV, with a weight of only 0.5 kg including GPS receiver, altimeter, wind speed sensor and a Canon IXUS 125 HS digital camera, automatically triggered for picture acquisition. The camera has a 16 megapixel CMOS sensor, capable of 4608 by 3456 pixels resolution with a 4:3 aspect ratio, and captures JPEG format images in the visible light range. The device operates in full-auto mode, including self-adjustment of aperture, ISO and shutter speed for the given light condition. In our survey, this resulted in ISO values in the range 100–500 and shutter speeds of 1/125–1/640 s with an aperture of $f/2.7$.

The survey took place on 28 August 2014, at approximately 8:20 AM. This time was chosen i) to avoid direct illumination of the glacier surface and thus a higher solar reflection which could saturate the pictures, and ii) to minimize wind speed that can cause staggering of the UAV and consequently produce blurred pictures (katabatic winds can occur along the Forni ablation tongue, see Senese & alii, 2012b; Gambelli & alii, 2014). Launch and landing location was set beside Rosole Lake at 2493 m a.s.l. (the yellow

dot in fig. 1b), close to Branca refuge and on the way to the glacier, and the maximum flight height was 250 m. The UAV was flown on the central and eastern parts of the tongue (see fig. 1b), for a total flight time of less than 30 minutes. The upper basins were not investigated due to UAV flight limitations, including battery life and line-of-sight operation and considering that reaching higher elevation in a short time could have entailed significant radial distortion in the acquired pictures. Images were processed via bundle block adjustment, including geometric correction to compensate for radial distortion in Menci APS software, to produce an orthomosaic with a ground resolution of 0.15 m x 0.15 m and a DEM with slightly lower resolution of 0.60 m x 0.60 m, to avoid gaps and artefacts generated by the stereo-matching process. In the absence of ground control points (GCPs), we estimated positional accuracy of the orthophoto and DEM to be about 3 m in the x and y coordinates, following Küng & alii (2011).

To compare this high-resolution image with a medium-resolution one, we obtained from USGS a Landsat 8 OLI/TIRS image acquired on 14/9/2014. This was the closest date of a Landsat overpass where the ablation tongue was free from cloud cover and shadows. We converted DN values (i.e. quantized and calibrated scaled Digital Numbers) to units of reflectance and brightness temperature using the coefficients found in the scene metadata (USGS, 2013). Geometric accuracy of the Landsat 8 OLI/TIRS sensors is estimated to be approximately 12 m (Storey & alii, 2014).

EXTRACTION OF GLACIER LARGE-SCALE FEATURES BASED ON THE UAV ORTHOMOSAIC

Concerning separability in the spectral domain, the medial moraines clearly stand out due to overall low values in all RGB channels of the orthomosaic, an effect that is also visible to a lesser degree on the Landsat image, caused by absorption of light at visible wavelengths by meltwater. Other features however are less distinct. In particular, the proglacial stream (i.e. Frodolfo stream) has similar spectral features as the glacier itself, with colors varying from a clear blue to almost saturation of the sensor, depending on water turbidity. Fine and sparse debris located on the tongue and on snow patches is also spectrally similar to proglacial debris.

In order to isolate large-scale features from the rest of the scene, we adopted a segmentation approach, identifying connected segments where pixels show similar spectral characteristics. This is in fact the recommended approach when dealing with high-resolution imagery, where objects to be identified are much larger than pixel size (Blaschke, 2010). We adopted different strategies to discriminate between features: the blue channel is ideal for identifying the glacier surface and the red channel for identifying the medial moraines.

EXTRACTION OF GLACIER LARGE-SCALE FEATURES BASED ON LANDSAT IMAGERY

To classify large-scale features of the Forni Glacier ablation tongue based on the Landsat OLI/TIRS image acquired on 14 September 2014, we employed optical and thermal information. First, we performed a supervised classification of the whole glacier surface using a stack of Landsat 8 bands, excluding band 1 (used for coastal aerosol detection), 8 (panchromatic) and 9 (cirrus detection), and including both thermal bands (i.e. 10 and 11). In particular, we defined training areas for the classification process by using the UAV image as a reference. Finally, by means of the shapefile created from the UAV orthomosaic, we selected the glacier ablation tongue on the Landsat image. This allowed a direct comparison between the two different approaches for identifying large-scale features: segmentation based on the UAV orthomosaic and supervised classification based on the Landsat OLI/TIRS image.

CLASSIFICATION OF THE GLACIER SMALL-SCALE FEATURES BASED ON THE UAV ORTHOMOSAIC

Once the glacier area was identified via segmentation, we attempted to further classify the different glacier surfaces by i) segmentation (i.e. snow, exposed ice, debris-rich ice, moraines, and water pond)

- ii) partitioning into different classes based on RGB values (i.e. debris free or debris covered ice)
- iii) Gabor filters (i.e. crevasses).

Concerning segmentation, given the differences in water color, no single spectral threshold could be used to extract all of the lakes, so they were identified separately. The largest lakes exhibit a greenish hue, likely due to a combination of suspended sediments and populations of algae that have colonized them (see also Boggero & *alii*, 2014). One example is the epiglacial pond on the eastern tongue, extracted based on the condition $green > red > blue$, whereas smaller ponds were identified via the blue channel. Snow patches featured different RGB values depending on clean and dirty snow, thus requiring two separate segmentation steps to identify them.

Concerning the second approach, an underlying assumption was made that over a glacier surface lower RGB values represent an increasing amount of fine debris deposition (in case of snow or ice), a wet surface (whenever water ponds occur) or shadows. In fact, localized shadow effects produced by surface topography at the time of image acquisition made it difficult to apply a single classification approach over the whole glacier surface. Over large areas, two pixels can feature a similar RGB value even if characterized by different surface conditions, e.g. one can be shadowed and the other one can feature a debris-covered surface. We therefore generated a hillshading map using the DEM extracted from the UAV survey (see section on Data Sources) and solar zenith and azimuth angles (Dozier & Frew, 1990) in order to identify an area with relatively uniform shadowing. We found that a limited part of the eastern tongue revealed these characteristics (red box in fig. 1b). Finally, we performed a decision-tree classification based on spectral properties in the RGB domain. This approach was chosen over supervised classification given the difficulty inherent in selecting homogeneous training areas.

Concerning crevasses, previous work on automatic delineation by Johannesson & *alii* (2011) was based on the local curvature of the ice surface obtained from a LiDAR digital elevation model (DEM). The photogrammetric DEM obtained from the UAV survey however was of insufficient resolution to test this method. In fact, most crevasses on the surface of the Forni Glacier that can be located on the orthomosaic are less than 0.50 m wide, whereas the resolution of the DEM was slightly coarser (0.60 x 0.60 m). Besides, photogrammetric DEM generation is known to be prone to errors in crevassed areas (Barrand & *alii*, 2009). The orthomosaic was therefore chosen to perform the detection. Our approach was based on Gabor filters, an image analysis technique for texture extraction that emphasizes linear features in an image, with tunable parameters of orientation, wavelength and frequency. In a glaciological context, Gabor filters have been used by Brenning & *alii* (2012) to map rock

glacier flow patterns. Here we used a bank of filters with 8 different orientations and wavelengths between 5 and 10 m. The analysis was performed using OpenCV implementation of Gabor filters, written in the Python programming language.

RESULTS AND DISCUSSION

IDENTIFICATION OF LARGE-SCALE FEATURES

Firstly, we identified the two large-scale features: the glacier area and the debris-ice transition zones (i.e. moraines). Based on the UAV orthomosaic, the glacier is easily separated from the rest of the scene (fig. 2) and when compared against visual assessment the approach identifies the terminus correctly, although misclassification occurs at the margins of the medial moraines. On the western part of the glacier tongue, a transition zone from glacier ice to medial moraine to lateral moraine is well visible (see also fig. 2) and the glacier margin is quite difficult to delimit correctly here. Slight overestimation of the glacier boundaries also occurs at the right margin of the eastern ice stream, because of fine debris located below a rock spur outside the glacier. Inclusion of morphometric parameters (such as slope and curvature) from the DEM in the classification process does not significantly improve the results. In fact, a DEM obtained via stereo-matching needs several images from different view angles and this does not occur at the margins. Therefore, the DEM quality decreases significantly along these areas (Küng & *alii*, 2011).

The segmentation process produces gaps in the final glacier and moraine segments due to very different RGB values compared to the neighboring pixels. On the upper parts of the moraines, these are mostly caused by isolated larger dry clasts not affected by meltwater, and thus possessing higher reflectance. Conversely on the actual glacier surface and on the terminal part of the eastern moraine, gaps appear as crevasses or at the debris/ice interface. If the final purpose is to produce a glacier map for inventories, it is recommended that these gaps should be removed via vector analysis. In this study however, they were included in the classification process. Isolated clasts can be considered as part of the medial moraine, and we included them in this category by performing neighborhood analysis, applying a 5x5 pixels neighborhood smoothing filter on unclassified data surrounded by medial moraine pixels. Conversely, gaps surrounded by glacier ice pixels were automatically assigned to the class debris-rich ice. This can leave clasts misclassified if larger than the filter size, and this issue could be solved using another segmentation step or individual correction to refine the overall classification.

To evaluate the advantages provided by the UAV orthoimage, we compared it to the classification based on medium-resolution data acquired by Landsat 8 (fig. 2 and tab. 1). Figure 2 shows the comparison between segmentation applied on UAV orthoimage (dark blue, yellow colours) and supervised classification using a combination of optical and thermal bands applied on Landsat 8 OLI/TIRS image (cyan, red colours). The higher resolution semi-automatic approach (based on the UAV orthoimage), even if using optical data alone, identifies the glacier surface better than the lower resolution method (based on the Landsat 8 image). In fact, through visual assessment we found that the latter misses the debris-covered sections of the glacier terminus and the terminal part of the western medial moraine. Another means of validating the accuracy of these approaches could consist in sampling reference points on the ground. However, this appears not necessary since the resolution of the UAV image is 0.15 m, much finer than the size of the large-scale features.

To better discriminate the medial moraines on the Landsat image, thermal bands could be excluded, because of their coarseness compared to optical bands. This way, however, relatively clean parts of the glacier would be classified as debris-covered.

Table 1 reports the areas of glacier features calculated from the final high- and medium-resolution classification maps: the total area of medial moraine pixels is very similar. Conversely, the medium-resolution-based approach underestimates the exposed ice area, as can be seen by looking at the eastern ice stream on Figure 2 and by considering the glacier ice area (Tab. 1). As a result, the total area occupied by the glacier in the Landsat based classification is also slightly lower. To evaluate the area estimation accuracy, we followed the methodology suggested by Vögtle & Shilling (1997) and applied among others by D'Agata & *alii* (2014), buffering the glacier perimeter to account for the sharpness of glacier limits, using a value of half the pixel size as the linear resolution error (O'Gorman, 1996). The uncertainty in the total area estimation from pixel resolution alone associated with a medium-resolution based classification is significantly larger (12 % compared to 0.002%), giving the limited size of the Forni glacier. Over short time scales, estimation of areal changes using medium-resolution tools like Landsat would thus be subject to an important noise component.

A direct comparison between the two approaches is only possible when considering large-scale features, since the small-scale ones, i.e. snow patches, epiglacial lakes and crevasses are smaller than a single pixel on the Landsat scene. Although fine debris is also not visible on the Landsat images, a shift towards lower reflectance values for ice is observable downglacier, especially closer to the terminus.

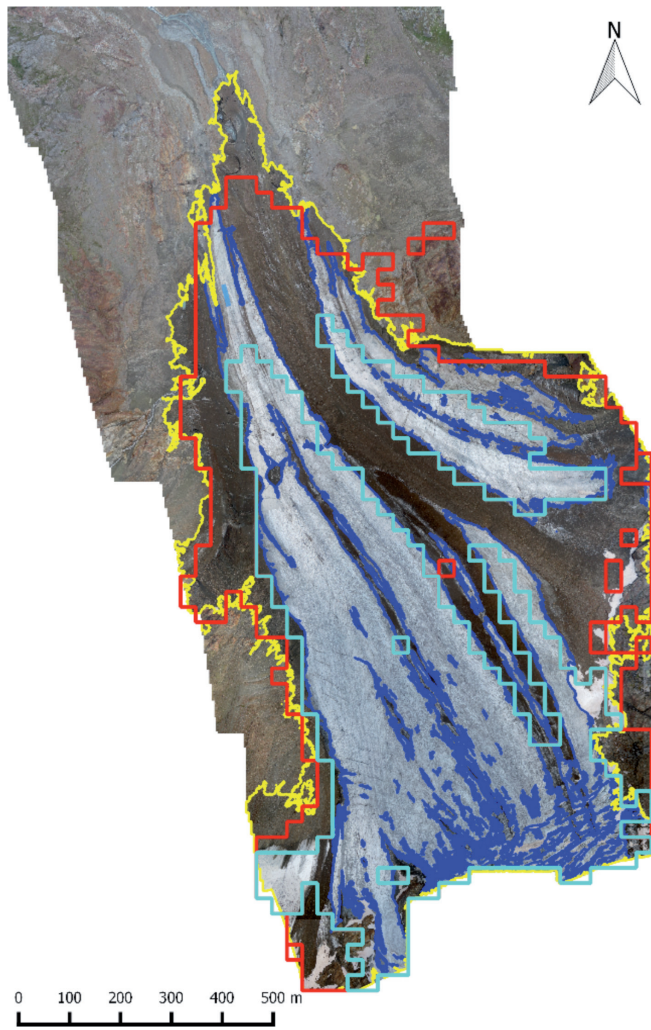


FIG. 2 - (Comparison between areas of bare ice and glacier perimeter derived from UAV-based (dark blue and yellow, respectively) and Landsat 8-based (light blue and red, respectively) classification. The base layer is the UAV image)

IDENTIFICATION OF SMALL-SCALE FEATURES BASED ON THE UAV ORTHOMOSAIC

Visual inspection of the entire UAV orthomosaic reveals many features not discernible on lower resolution images, namely: i) snow patches prominent on the upper parts (rela-

tive to the study area) of the eastern and central ice streams; ii) fine and sparse debris patches and debris bands located on the glacier surface; iii) the debris cone on the central part of the tongue; iv) the supraglacial pond located on the eastern part of the tongue and the small lake at the take-off site (Rosole Lake), as well as smaller scattered proglacial and epiglacial ponds; and v) longitudinal and transverse crevasses widespread on the glacier surface, especially the eastern ice stream.

The final map produced by the segmentation approach is shown in Figure 3. Slight misclassification errors occurred for dirty snow, as some patches were missed by the segmentation approach because of insufficient contrast with the surrounding terrain. For this reason, snow patches are displayed in purple in Figure 3, not distinguishing between clean and dirty ones, and they cover 25132 m² (Tab. 3). Unlike snow, the ice surfaces were well detected, and labelled differently whether partially or completely debris-covered (yellow and brown pixels, respectively) or debris-free (cyan pixels). As expected along the ablation tongue in August, the glacier ice (cyan pixels) covers a wider area compared to snow (45.66% and 2.58%, respectively, Tab. 2). Like the medial moraines, the small neo-moraines are correctly identified by the segmentation approach. In addition, the terminal part of the eastern medial moraine results correctly characterized by a mix of supraglacial debris (brown pixels), debris-rich ice (yellow pixels) and epiglacial lakes (blue pixels). In fact, recently the glacier has undergone very intense dynamic processes, compromising surface stability and causing enlargement of crevasses especially along the eastern tongue, and collapse of other areas. An example of the latter is indeed found on the terminal part of the eastern medial moraine (visible as cyan pixels in fig. 3). As an evidence of the darkening phenomena reported by previous studies (Diolaiuti & Smiraglia, 2010; D'Agata & *alii*, 2014), the supraglacial debris covers a similar area with respect to the glacier ice (i.e. ca. 46%, Tab. 2). Moreover, the large pond located at the margin of the eastern ice stream is correctly identified compared to visual assessment, with an area of 309.23 m², and the two smaller ponds at the frontal glacier margin are properly recognized as well. The total area of epiglacial lakes covers 841 m² (blue pixels in fig. 3, see also Tab. 2).

TABLE 1 - Comparison between areas resulting from high- and medium-resolution classification of the Forni Glacier ablation tongue.

Category	UAV-based classification		Landsat 8 -based classification		Δ area (Landsat 8 -UAV)
	Area (m ²)	Area (%)	Area (m ²)	Area (%)	Area (m ² and %)
Glacier ice	512870 ± 0.006%	53.93	496568 ± 24%	52.48	-16302 or - 3.2%
Moraines	448036 ± 0.006%	46.07	449571 ± 24%	47.52	+1535 or + 0.34%
Total	960906 ± 0.002%	100.00	946139 ± 12%	100.00	-14767 or - 1.5%

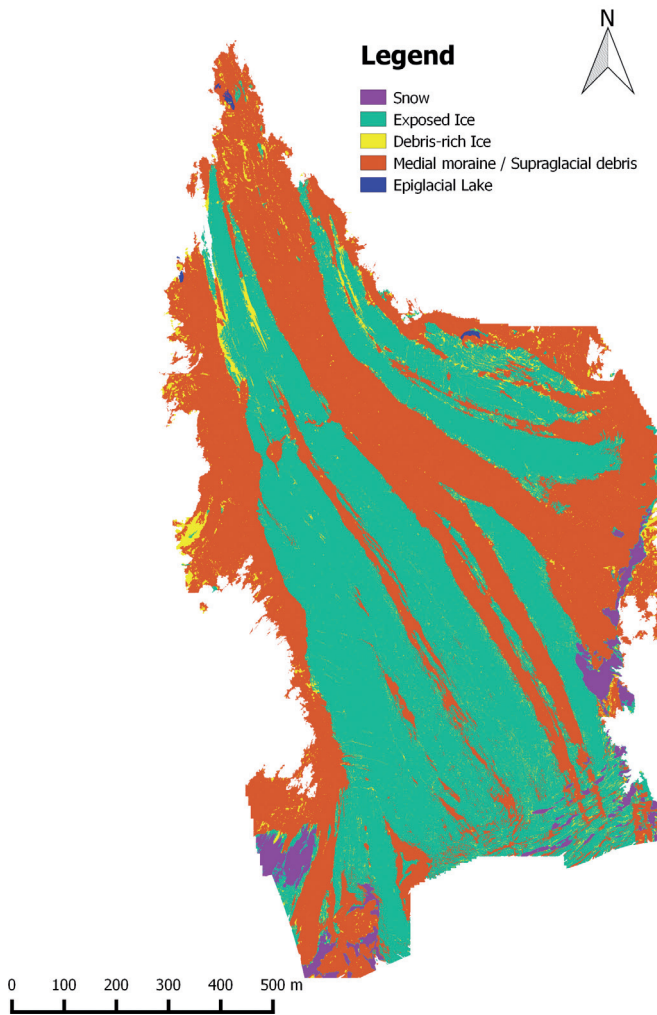


FIG. 3 - Segmentation-based classification of UAV orthoimage of the ablation tongue of the Forni Glacier.

TABLE 2 - Area values covered by small-scale features resulting from high-resolution classification of the Forni Glacier ablation tongue

Category	UAV-based classification	
	Area (m ²)	Area (%)
Snow	25132	2.58
Debris-Free Ice	453841	46.66
Debris-Rich Ice	33058	3.40
Moraines	448036	46.07
Lakes	841	0.09

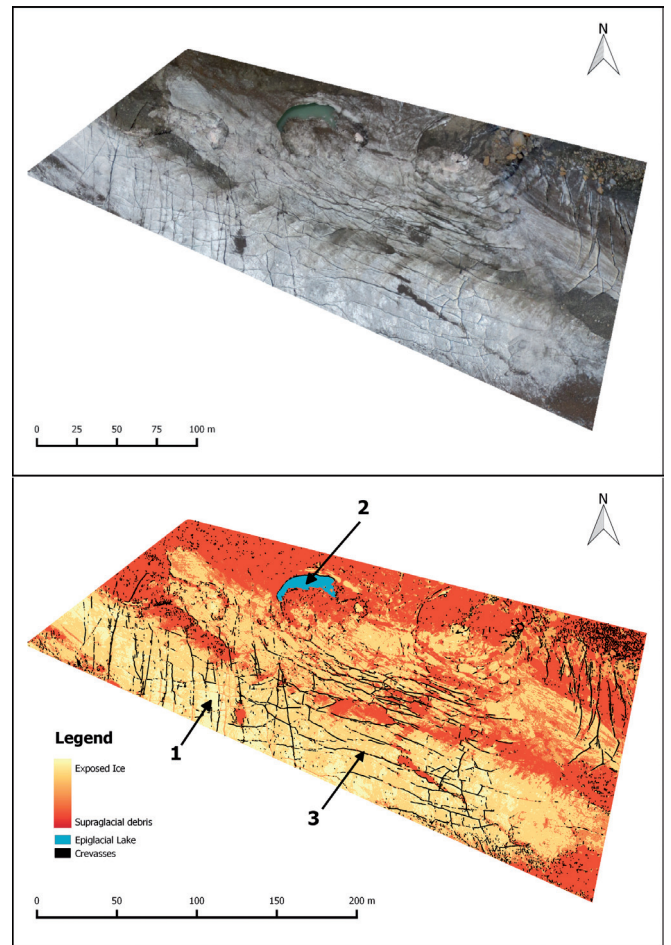


FIG. 4 - (A) Original UAV orthoimage and (B) classified test area for fine debris occurrence, from exposed ice to supraglacial debris (red color scale). Crevasses are also shown in black and the large epiglacial lake in blue. With the numbers 1 to 3 are displayed examples of exposed ice, epiglacial lake and crevasses, respectively.

Finally, we applied the Gabor filter over the whole UAV orthoimage (not shown). The largest number of crevasses is recognized when using a low wavelength value of 5 m, consistent with the spacing of crevasses on the glacier surface. However, a significant number of false positives is also produced, mostly due to shadows projected by larger clasts that appear as linear features. Overall, the approach showed promising results. As suggested by Brenning & *alii* (2012), further research aimed at improving the classification should combine different methodologies, including other texture measures or terrain parameters (i.e. local curvature) to filter out unwanted shadow effects.

A more detailed analysis was performed over an area with relatively uniform shadowing along the eastern ablation tongue (47544 m², fig. 4). There, in addition to the

delineation of water ponds and crevasses, fine debris cover is more deeply analyzed. In this area, debris supply comes mostly from macrogelivation and rock degradation processes (Azzoni & *alii*, 2014) and a transition from supraglacial debris (i.e. buried-ice) to exposed ice (i.e. bare-ice) is well discerned away from the margin towards the center (lower part of both the images in fig. 4). Here, the darkening phenomena are even more evident compared to the picture showing the entire tongue (fig. 3): the bare-ice pixels are 7.49% of the total excluding water pond and crevasses. The area is also heavily crevassed and here application of the Gabor filter is particularly successful (black pixels in fig. 4). This is a consequence of uniform illumination restricting the range of RGB values, although some sections are still missed because of lack of contrast. As expected the water pond is also well identified. The analysis shown in Figure 4 is a further proof of the intensity of the recent glacier dynamics. In fact, in spite of crevasses covering only 2.79% of the total investigated area, the surface appears very fragmented due to their wide spatial distribution. In addition, the water pond was likely created by a significant collapse.

CONCLUSIONS

The methodology presented here shows that it is possible to provide high-resolution mapping of a glacier using a semi-automatic approach based on uncalibrated RGB data, obtained with a low cost on-demand UAV survey, with an accuracy comparable or higher than when using medium-resolution satellite data. Large-scale features (i.e. exposed glacier surface and medial moraines) could be easily identified using this approach, with only slight misclassification at the margins of the medial moraines. This suggests that for the purpose of generating glacier inventories a segmentation step based on high-resolution orthoimagery (from UAV or conventional aerial surveys) could speed up delineation of glacier boundaries especially on debris free glaciers. Another significant advantage of a high-resolution approach is the decrease in uncertainty related to pixel size, potentially enabling estimation of areal changes over short periods. Classification of debris-covered glaciers with different lithology and morphology of debris cover remains to be tested, although the capability of UAVs to carry different payloads means that different data sets, including near infrared, thermal and morphometric data could be used to improve accuracy of the results. The inclusion of these data sets could also lead to faster algorithms. In fact, compared with coarser resolution approaches, the methodology we proposed requires considerable user input for threshold selection and manual checking of the segments.

An important improvement over medium-resolution based classification is the ability to map smaller geomorphological features, including snow coverage, epiglacial lakes

and crevasses. For the latter, a new approach was presented here based on Gabor filters, which showed promising results. Continuous mapping of these features can inform the local communities, as these features can represent a hazard, and give important clues as to the evolution of the glacier and the magnitude of the stresses acting upon the surface.

Our findings represent a further proof of the general darkening phenomena occurring at the Alpine debris-free glaciers (Oerlemans & *alii*, 2009; Diolaiuti & Smiraglia, 2010) and in particular at the Forni Glacier tongue (D'Agata & *alii*, 2014). Indeed, we found that the bare-ice surfaces cover a similar area compared to the buried-ice ones. In addition, the intensity of recent glacier dynamics and the resulting surface instability is evident in the mapped morphologies such as crevasses (2.79% of the total area investigated in detail) and water ponds.

UAV-based remote sensing is still explorative, and at present there is a lack of standard procedures for correct calibration of the data, when they are used to estimate physical quantities (e.g. reflectance) rather than for qualitative assessment such as mapping. As an example, in our research we found the shadowing effect of local topography and geometry of the illumination to be important factors in driving the final RGB values of the orthomosaic. This prevented further classification of fine debris glacier-wide, and although these issues have been tackled for spaceborne sensors, the algorithms will have to be adapted for the platform shift.

Another critical issue of UAV-based remote sensing, also noted by Whitehead & *alii* (2013), is that limitations imposed by battery life and line-of-sight operation currently restrict flight time, so that for instance an entire survey of the Forni Glacier would have required multiple flights. However, this is the largest valley glacier in the Italian Alps, where instead smaller glaciers are predominant. Since small glaciers are more likely to be inaccurately classified when using lower resolution data and have been shown to react strongly to climate change (e.g. D'Agata & *alii*, 2014; Diolaiuti & *alii*, 2012), the introduction and improvement of low-cost mapping methods can make an important contribution to Alpine glaciological and geomorphological studies.

REFERENCES

- AZZONI R.S., SENESE A., ZERBONI A., MAUGERI M., SMIRAGLIA C. & DIOLAIUTI G. (2014) - *A novel integrated method to describe dust and fine supraglacial debris and their effects on ice albedo: the case study of Forni Glacier, Italian Alps*. The Cryosphere Discuss, 8, 3171-3206
- BARRAND N.E., MURRAY T., JAMES T.D., BARR S.L. & MILLS J.P. (2009) - *Optimizing photogrammetric DEMs for glacier volume change assessment using laser-scanning derived ground-control points*. Journal of Glaciology, 55, 106-116
- BENN D.I., BOLCH T., HANDS K., GULLEY J., LUCKMAN A., NICHOLSON L.I., QUINCEY D., THOMPSON S., TOUMI R. & WISEMAN S. (2012) - *Response of debris-covered glaciers in the Mount Everest region to recent warm-*

- ing, and implications for outburst flood hazards. *Earth Science Reviews*, 114, 156-174
- BLASCHKE T. (2010) - *Object-based image analysis for remote sensing*. ISPRS Journal of Photogrammetry and Remote Sensing, 65, 2-16
- BOGGERO A., ROGORA M., MUSAZZI S., ZAUPA S., LAMI A., SALERNO F., GUZZELLA L., GAMBELLI S., GUYENNON N., VIVIANO G., THAKURI S. & TARTARI G. (2013) - *Un Mondo D'acqua In Alta Quota. Le acque del Parco Nazionale dello Stelvio, un laboratorio a cielo aperto per lo studio dei cambiamenti climatici*. Ed. Associazione Comitato Ev-K2-CNR, 91 pp.
- BRENNING A., LONG S. & FIEGUTH P. (2012) - *Detecting rock glacier flow structures using Gabor filters and IKONOS imagery*. *Remote Sensing of Environment*, 125, 227-237
- D'AGATA C., BOCCHIOLA D., MARAGNO D., SMIRAGLIA C. & DIOLAIUTI G. (2014) - *Glacier shrinkage driven by climate change during half a century (1954–2007) in the Ortles-Cevedale group (Stelvio National Park, Lombardy, Italian Alps)*. *Theory of Applied Climatology*, 116, 169-190
- DIOLAIUTI G., BOCCHIOLA D., D'AGATA C., & SMIRAGLIA C. (2012) - *Evidence of climate change impact upon glaciers' recession within the Italian alps: the case of Lombardy glaciers*. *Theoretical and Applied Climatology*, 109, 429-445
- DIOLAIUTI G. & SMIRAGLIA C. (2010) - *Changing glaciers in a changing climate: how vanishing geomorphosites have been driving deep changes in mountain landscapes and environments*. *Géomorphologie : relief, processus, environnement*, 2, 131-152
- DOZIER J. & FREW J. (1990) - *Rapid Calculation of Terrain Parameters For Radiation Modeling From Digital Elevation Data*. *IEEE Transactions on Geoscience and Remote Sensing*, 28, 963-969
- EEA (EUROPEAN ENVIRONMENT AGENCY) (2012) - *Climate change, impacts and vulnerability in Europe 2012*. http://www.eea.europa.eu/publications/climate-impacts-and-vulnerability-2012/at_download/file
- FISCHER M., HUSS M., BARBOUX C. & HOELZLE M. (2014) - *The new Swiss Glacier Inventory SGI2010: relevance of using high-resolution source data in areas dominated by very small glaciers*. *Arctic, Antarctic and Alpine Research*, 46, 933–945
- GAMBELLI S., SENESE A., D'AGATA C., SMIRAGLIA C. & DIOLAIUTI G. (2014) - *Distribution of the surface Energy budget: preliminary analysis on the incoming solar radiation. The case study of the Forni Glacier (Italy)*. *Geografia Fisica e Dinamica Quaternaria*, 37, 15-22.
- HODSON A., ANESIO A.M., NG F., WATSON R., QUIRK J., IRVINE-FYNN T., DYE A., CLARK C., MCCLOY P., KOHLER J. & SATTLER B. (2007) - *A glacier respire: Quantifying the distribution and respiration CO2 flux of cryoconite across an entire Arctic supraglacial ecosystem*. *Journal of Geophysical research*, 112, 1-9
- IMMERZEEL W.W., KRAAIJENBRINK P.D.A., SHEA M. J., SHRESTHA A.B., PELLICCIOTTI F., BIERKENS M.F.P. & DE JONG S.M. (2014) - *High-resolution monitoring of Himalayan glacier dynamics using unmanned aerial vehicles*. *Remote Sensing*, 150, 93-103
- JOHANNESSON T., BJORNSSON H., PALSSON F., SIGURDSSON O. & ÞORSTEINSSON P. (2011) - *LiDAR mapping of the Snæfellsjökull ice cap, western Iceland*. *Jokull*, 61, 19-32
- KNOLL C. & KERSCHNER H. (2009) - *A glacier inventory for South Tyrol, Italy, based on airborne laser-scanner data*. *Annals of Glaciology*, 50, 46-52
- KÜNG O., STRECHA C., BEYELER A., ZUFFEREY J.C., FLOREANO D., FUA P. & GERVAIX F. (2011) - *The Accuracy Of Automatic Photogrammetric Techniques On Ultra-Light Uav Imagery*. 38, *International Archives of the Photogrammetry, Remote Sensing and Spatial Information Sciences, Conference on Unmanned Aerial Vehicle in Geomatics, Zurich, Switzerland*
- OERLEMANS J., GIESEN R.H. & VAN DEN BROEKE M.R. (2009) - *Retreating alpine glaciers: increased melt rates due to accumulation of dust (Vadret da Morteratsch, Switzerland)*. *Journal of Glaciology*, 55, 729-736
- O'GORMAN L. (1996) - *Subpixel precision of straight-edged shapes for registration and measurement*. *IEEE Transactions on Pattern Analysis and Machine Intelligence*, 18, 746-751
- PAUL F., BARRAND N.E., BAUMANN S., BERTHIER E., BOLCH T., CASEY K., FREY H., JOSHI S.P., KONOVALOV V., LE BRIS N., MOLG N., NOSENKO G., NUTH C., POPE A., RACOVITANU A., RASTNER P., RAUP B., SCHARRER K., STEFFEN S. & WINSVOLD S. (2013) - *On the accuracy of glacier outlines derived from remote-sensing data*. *Annals of Glaciology*, 54, 171-182
- RYAN J.C., HUBBARD A.L., BOX J.E., TODD J., CHRISTOFFERSEN P., CARR J.R., HOLT T.O. & SNOOKE N. (2015) - *UAV photogrammetry and structure from motion to assess calving dynamics at Store Glacier, a large outlet draining the Greenland ice sheet*. *The Cryosphere*, 9, 1-11
- SENESE A., DIOLAIUTI G., MIHALCEA C. & SMIRAGLIA C. (2012a) - *Energy and mass balance of Forni Glacier (Stelvio National Park, Italian Alps) from a 4-year meteorological data record*. *Arctic, Antarctic, and Alpine Research*, 44, 122-134
- SENESE A., DIOLAIUTI G., VERZA G.P. & SMIRAGLIA C. (2012b) - *Surface energy budget and melt amount for the years 2009 and 2010 at the Forni Glacier (Italian Alps, Lombardy)*. *Geografia Fisica e Dinamica Quaternaria*, 35, 69-77
- SHUKLA A., ARORA M.K. & GUPTA R. P. (2010) - *Synergistic approach for mapping debris-covered glaciers using optical-thermal remote sensing data with inputs from geomorphometric parameters*. *Remote Sensing of Environment*, 114, 1378-1387
- SMIRAGLIA C. (1989) - *The Medial moraines of Ghiacciaio dei Forni, Valtellina, Italy: morphology and sedimentology*. *Journal of glaciology*, 35, 81-84
- STOREY J., CHOATE M. & LEE K. (2014) - *Landsat 8 Operational Land Imager On-Orbit Geometric Calibration and Performance*. *Remote sensing*, 6, 11127-11152
- USGS (UNITED STATES GEOLOGICAL SURVEY) (2013) - *Using the USGS Landsat 8 Product*. Available at: http://landsat.usgs.gov/Landsat8_Using_Product.php, Last Accessed 17/5/2013
- VÖGTLE T. & SCHILLING K. J. (1999) - *Digitizing Maps*. In: BÄHR H.-P. & VÖGTLE T. (eds.), «GIS for Environmental Monitoring», Stuttgart, Schweizerbart, 201-216.
- WHITEHEAD K., MOORMAN B.J. & HUGENHOLTZ C.H. (2013). *Brief Communication: Low-cost, on-demand aerial photogrammetry for glaciological measurement*. *The Cryosphere*, 7, 1879-1884

(Ms received 1 March 2015; Accepted 1 June 2015)

